Magn Reson Med Sci 2021; 20; 69–75
doi:10.2463/mrms.mp.2019-0151
Published Online: March 12, 2020

MAJOR PAPER

Comparison of the Diagnostic Value of Mono-exponential, Bi-exponential, and Stretched Exponential Signal Models in Diffusion-weighted MR Imaging for Differentiating Benign and Malignant Hepatic Lesions

Yoshifumi Noda[1*], Satoshi Goshima[2], Keita Fujimoto[1], Yuta Akamine[3], Kimihiro Kajita[1], Nobuyuki Kawai[1], and Masayuki Matsuo[1]

Purpose: To compare the diagnostic value of mono-exponential, bi-exponential, and stretched exponential diffusion-weighted imaging (DWI) for differentiating benign and malignant hepatic lesions.

Methods: This prospective study was approved by our Institutional Review Board and the patients provided written informed consent. Magnetic resonance imaging was acquired for 56 patients with suspected liver disease. This identified 90 focal liver lesions with a maximum diameter >10 mm, of which 47 were benign and 43 were malignant. Using home-built software, two radiologists measured the DWI parameters of hepatic lesions for three models: the apparent diffusion coefficient (ADC) from a mono-exponential model; the true diffusion coefficient (D), pseudo-diffusion coefficient (D^*), and perfusion fraction (f) from a bi-exponential model; and the distributed diffusion coefficient (DDC) and water molecular diffusion heterogeneity index (α) from a stretched exponential model. The parameters were compared between benign and malignant hepatic lesions.

Results: ADC, D, D^*, f, and DDC values were significantly lower for malignant hepatic lesions than for benign lesions ($P < 0.0001$–0.03). Although logistic regression analysis demonstrated that DDC was the only statistically significant parameter for differentiating benign and malignant lesions ($P = 0.039$), however, the areas under the receiver operating characteristic curve for differentiating benign and malignant lesions were comparable between ADC (0.98) and DDC (0.98) values.

Conclusion: DDC values obtained from the stretched exponential model could be also used as a quantitative imaging biomarker for differentiating benign and malignant hepatic lesions, however, the diagnostic performance was comparable with ADC values.

Keywords: *magnetic resonance imaging, liver neoplasms, abdomen*

Introduction

With the current widespread use of imaging, it is common to encounter focal hepatic lesions in routine clinical practice. Diffusion-weighted imaging (DWI) is increasingly used for the detection and characterization of such lesions.[1] DWI reflects the diffusibility of water molecules within tissues, with this characteristic typically quantified using the apparent diffusion coefficient (ADC) calculated using a mono-exponential model. Although ADC value have the potential to be used to differentiate benign and malignant hepatic lesions, there can be a considerable overlap in the ADC values of these two types of lesion.[2,3] ADC values are affected by both molecular diffusion and blood perfusion, so they do not represent true tissue characteristics.[4] In contrast, intravoxel incoherent motion (IVIM) calculated from a bi-exponential model with multiple b-values can theoretically separate the perfusion components from the true diffusion of water molecules, allowing the quantification of three parameters: the true diffusion coefficient (D), the pseudo-diffusion coefficient (D^*), and the perfusion fraction (f). Recently,

[1]Department of Radiology, Gifu University, Gifu, Japan
[2]Department of Diagnostic Radiology & Nuclear Medicine, Hamamatsu University, Shizuoka, Japan
[3]Philips Japan, Tokyo, Japan
[*]Corresponding author: Department of Radiology, Gifu University, 1-1 Yanagido, Gifu, Gifu 501-1194, Japan. Phone: +81-58-230-6437, Fax: +81-58-230-6440, E-mail: noda1031@gifu-u.ac.jp

Received: October 24, 2019 | Accepted: February 8, 2020

some studies demonstrated the utility of bi-exponential model for differentiating benign and malignant tissues.[5–8] However, tumor tissue and its microstructure are complex and varied, and it can be less than ideal to characterize them using only two intravoxel proton pools, as in the bi-exponential model. To overcome this limitation of bi-exponential models, a stretched exponential model has been introduced.[9] The stretched exponential model is indicated to reflect physiologic characteristics of biologic tissue, heterogeneity of intravoxel diffusion rates, and the distributed diffusion effect within each voxel in multiple pools of water molecules.[9] This quantifies the intravoxel heterogeneity using two parameters: the distributed diffusion coefficient (DDC) and intravoxel water diffusion heterogeneity (α).

The aim of this study was to compare the diagnostic value of the mono-exponential, bi-exponential, and stretched exponential DWI models for differentiating benign and malignant hepatic lesions.

Materials and Methods

Patients

Our Institutional Review Board approved this prospective study and written informed consent was obtained from all the patients. Between August 2018 and January 2019, 140 consecutive patients with known or suspected liver disease, based either on their clinical history or on previously performed computed tomography, underwent gadoxetic acid-enhanced magnetic resonance imaging (MRI). Of these, 84 patients were excluded based on the following exclusion criteria: maximum diameter of the hepatic lesion <10 mm (n = 45); no hepatic lesion (n = 33); a hepatic lesion undetectable on the DWI map (n = 4); and no histopathological diagnosis (n = 2). The remaining 56 patients (mean age, 65.7 ± 14.1 years; age range, 26–87 years) were included in our study. Of these, 34 were men (mean age, 67.6 ± 12.8 years; age range, 26–85 years) and 22 were women (mean age, 62.8 ± 15.7 years; age range, 35–87 years).

Diagnosis of the focal hepatic lesions

The hepatic lesions were diagnosed based on typical clinical and MRI findings with at least 6 months of follow-up. The diagnostic MRI criteria for the focal hepatic lesions were as follows: hepatocellular carcinoma (HCC), exhibiting arterial hyperenhancement and venous or delayed phase washout in high-risk patients, according to the criteria proposed by the American Association for the Study of Liver Disease;[10] liver metastasis, exhibiting peripheral rim enhancement and an increase in diameter of at least 20% during serial imaging follow-up in patients with a known primary malignancy;[11] early HCC (eHCC), exhibiting no dominant arterial blood supply, fat-containing, hyper- or iso- to hypointense to liver parenchyma on T_2-weighted images, and with low signal intensity on gadoxetic acid-enhanced MRI obtained in the portal venous, late, and hepatocyte phases;[12] hemangioma, exhibiting high signal intensity on T_2-weighted images and a typical dynamic enhancement pattern without interval change; a cyst, exhibiting bright signal intensity on T_2-weighted images and no contrast enhancement;[6] focal nodular hyperplasia (FNH), exhibiting strong arterial hyperenhancement, the retention of contrast agent on hepatobiliary phase images, and a hyperintense central scar on T_2-weighted images;[13] and an abscess, exhibiting peripheral enhancing multiseptated cystic lesions in a clinical setting, with fever and chills.[14]

MRI protocol

Magnetic resonance imaging was acquired using a 3T MR system (Ingenia 3T CX; Philips Medical Systems, Best, The Netherlands) equipped with a 32-channel digital coil. Free-breathing, two-dimensional fat-suppressed axial DWI was acquired with a single-shot echo planar sequence using the following parameters: TR/TE, 5000/57 ms; field of view, 40 × 32 cm; matrix, 96 × 96; parallel imaging factor, 2.0; slice thickness/gap, 6/1; slice number, 30 slices; b-values, 0, 10, 25, 50, 75, 100, 200, 500, and 800 s/mm^2; and acquisition time, 4 min 15 s. The remaining MRI protocols comprised the following sequences: in-phase and opposed-phase T_1-weighted axial gradient recalled echo imaging; respiratory-triggered, two-dimensional, fat-suppressed axial T_2-weighted turbo spin-echo imaging; and breath-hold, three-dimensional, fat-suppressed, spoiled fast field echo, axial gadoxetic acid-enhanced imaging of the hepatic arterial dominant, portal venous, late dynamic, and hepatobiliary phases.

Postprocessing and analysis of DWI data

The DWI data were postprocessed using home-built software (EXPRESS 2.0, Philips Healthcare, Korea) to calculate the DWI parameters. These were based on the following mathematical models: $S(b)$, signal intensity at a particular b-value; and S_0, signal intensity without a diffusion gradient. All nine b-values were used as input data.

Apparent diffusion coefficient values were calculated using the mono-exponential linear fitting technique according to the following equation:

$$\frac{S(b)}{S_0} = \exp(-b \times \mathrm{ADC})$$

In the bi-exponential model, the IVIM parameters were calculated using the following equation:[15]

$$\frac{S(b)}{S_0} = \left[(1-f) \times \exp(-b \times D)\right] + \left[f \times \exp(-b \times D^*)\right]$$

D was calculated using a simple linear fit equation with b-values >200 s/mm^2, and D^* and f were calculated using a nonlinear regression algorithm.

In the stretched exponential model, DDC and α were calculated using the following equation:[9]

$$\frac{S(b)}{S_0} = \exp[-(b \times \mathrm{DDC})]^{\alpha}$$

where DDC is the mean intravoxel diffusion rate and α is the intravoxel water molecular diffusion heterogeneity.

The DWI image analyses were performed by two radiologists (N.K., and K.F., with 10 and 6 years of post-training experience in interpreting abdominal MR images, respectively), who were blinded to the patients' clinical information. Regions of interest were drawn manually to encompass entire the hepatic lesions, while consulting the other MR images to guarantee the detection of the lesions. The DWI parameters were then automatically calculated and the radiologists recorded these values.

Statistical analysis

MedCalc Statistical Software for Windows version 19.1.5 (MedCalc Software, Mariakerke, Belgium) was used for all the statistical analyses. The Mann–Whitney *U* test was applied to evaluate differences in DWI parameters between benign and malignant hepatic lesions. The optimal threshold for each parameter for differentiating between benign and malignant hepatic lesions was determined based on the highest area under the receiver operating characteristic (ROC) curve (AUC) that yielded the highest sensitivity and specificity. The DWI parameters were evaluated by comparing the associated AUCs, using the method of Hanley and McNeil.[16] The statistically significant DWI parameters were included in stepwise logistic regression analysis to differentiate between benign and malignant hepatic lesions. Interobserver variability in the DWI parameters were assessed using the intraclass correlation coefficient (ICC), which measure the degree of consensus between two radiologists. An ICC of ≤0.20 was interpreted as slight agreement, 0.21–0.40 as fair agreement, 0.41–0.60 as moderate agreement, 0.61–0.80 as substantial agreement, and ≥0.81 as almost perfect agreement. A *P*-value of <0.05 was considered to be statistically significant.

Results

Focal hepatic lesions

In total, 90 focal hepatic lesions were evaluated in 56 patients. Of these, 47 lesions were benign (mean maximum diameter, 40.5 ± 27.7 mm; range, 10.4–132.9 mm). These included simple cysts (n = 24), hemangiomas (n = 11), complicated cysts (n = 5), FNHs (n = 4), and abscesses (n = 3). The 43 malignant hepatic lesions (mean maximum diameter, 28.8 ± 19.4 mm; range, 10.7–120.1 mm) included liver metastasis (n = 23), HCC (n = 19), and eHCC (n = 1). Table 1 lists the mean maximum diameters for each type of hepatic lesion.

Analysis of DWI data

Table 2 compares the DWI parameters between the benign and malignant hepatic lesions. Values for the following parameters were significantly lower for malignant than for benign hepatic lesions: ADC (P < 0.0001), D (P < 0.0001),

Table 1 Benign and malignant hepatic lesions

Focal hepatic lesions	Number	Mean maximal diameter (mm)
Benign		
Simple cyst	24	40.0 ± 24.6 (10.4–85.7)
Hemangioma	11	28.6 ± 18.9 (12.8–77.9)
Complicated cyst	5	69.3 ± 20.5 (17.0–132.9)
Focal nodular hyperplasia	4	42.6 ± 14.1 (26.3–60.5)
Abscess	3	18.2 ± 11.6 (11.0–31.6)
Malignant		
Metastasis	23	31.5 ± 13.0 (10.7–73.4)
Hepatocellular carcinoma	19	26.2 ± 25.4 (12.0–120.1)
Early hepatocellular carcinoma	1	16.0

Data are means ± 1 standard deviation. Numbers in parentheses are ranges.

Table 2 Diffusion-weighted imaging parameters between benign and malignant hepatic lesions

	Benign (n = 47)	Malignant (n = 43)	ICC	P value
ADC (×10^{-3} mm^2/s)	2.83 ± 1.05 (1.14–6.64)	1.09 ± 0.32 (0.39–2.42)	0.87	<0.0001*
IVIM D (×10^{-3} mm^2/s)	2.44 ± 0.84 (1.11–4.37)	0.98 ± 0.39 (0.0–2.27)	0.86	<0.0001*
IVIM D^* (×10^{-3} mm^2/s)	113.6 ± 76.9 (1.0–200.0)	80.1 ± 78.5 (2.6–200.0)	0.59	0.030*
IVIM f (%)	25.1 ± 25.0 (0.0–100.0)	17.5 ± 22.5 (0.0–100.0)	0.42	0.021*
DDC (×10^{-3} mm^2/s)	3.00 ± 1.22 (1.14–7.20)	1.03 ± 0.35 (0.18–2.45)	0.94	<0.0001*
α	0.74 ± 0.25 (0.07–1.0)	0.80 ± 0.22 (0.25–1.0)	0.73	0.14

*P < 0.05, significant difference. Data are means ± 1 standard deviation. Numbers in parentheses are ranges. ADC, apparent diffusion coefficient; IVIM, intravoxel incoherent motion; f, perfusion fraction; D^*, pseudodiffusion coefficient; D, true diffusion coefficient; DDC, distributed diffusion coefficient; α, intravoxel water diffusion heterogeneity; ICC, intraclass correlation coefficient.

Table 3 Diagnostic performance for differentiating benign and malignant hepatic lesions

	Cut-off value	Sensitivity (%)	Specificity (%)	AUC (95% CI)
ADC ($\times 10^{-3}$ mm^2/s)	1.46	97.7	92.9	0.979 (0.921–0.998)
IVIM D ($\times 10^{-3}$ mm^2/s)	1.40	95.3	93.2	0.965 (0.901–0.993)
IVIM D^* ($\times 10^{-3}$ mm^2/s)	76.6	65.1	61.4	0.629 (0.517–0.731)
IVIM f (%)	21.3	81.4	43.2	0.605 (0.493–0.709)
DDC ($\times 10^{-3}$ mm^2/s)	1.46	97.7	93.2	0.980 (0.923–0.998)
α	0.57	86.0	31.8	0.549 (0.438–0.657)

ADC, apparent diffusion coefficient; IVIM, intravoxel incoherent motion; f, perfusion fraction; D^*, pseudodiffusion coefficient; D, true diffusion coefficient; DDC, distributed diffusion coefficient; α, intravoxel water diffusion heterogeneity; CI, confidence interval.

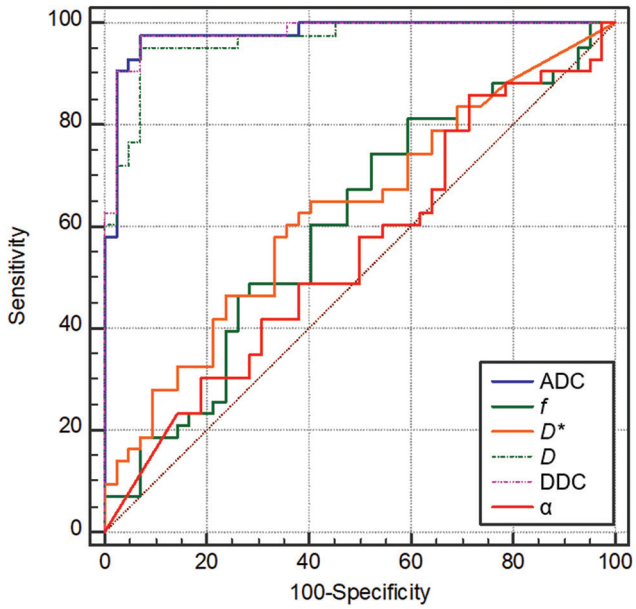

Fig. 1 Receiver operating characteristic (ROC) curves for differentiating benign and malignant hepatic lesions. The largest area under the ROC curve was for DDC (0.980, 95% confidence interval 0.923–0.998), followed by ADC, D, D^*, f, and α. DDC, distributed diffusion coefficient; ADC, apparent diffusion coefficient.

D^* ($P = 0.030$), f ($P = 0.021$), and DDC ($P < 0.0001$). There was no significant difference in α between the benign and malignant hepatic lesions ($P = 0.14$). Interobserver reproducibility of the measurements of DWI parameters were moderate to almost perfect agreement (ICC, 0.42–0.94).

Table 3 summarizes the results of the ROC analyses for differentiating benign and malignant lesions. Among the DWI parameters, DDC values showed the largest AUC [0.980, 95% confidence interval (CI) 0.923–0.998] followed by ADC, D, D^*, f, and α. The AUC for DDC value was significantly larger value than those for D^* ($P < 0.0001$), f ($P < 0.0001$), and α ($P < 0.0001$). The AUC for ADC value was significantly larger than those for D^* ($P < 0.0001$), f ($P < 0.0001$), and α ($P < 0.0001$), and the AUC values for D was significantly larger than those for f ($P < 0.0001$) and α ($P < 0.0001$) (Fig. 1). The logistic regression analysis demonstrated that only DDC values was a significant parameter for differentiating benign and malignant lesions ($P = 0.039$). Table 4 and Figs. 2–4 show the DDC values for each type of focal hepatic lesion.

Table 4 DDC of each focal hepatic lesions

Hepatic lesions	DDC ($\times 10^{-3}$ mm^2/s)
Simple cyst	3.52 ± 1.02 (2.22–7.20)
Complicated cyst	2.49 ± 0.83 (1.14–3.34)
Abscess	2.40 ± 0.56 (1.78–2.84)
Hemangioma	2.87 ± 1.58 (1.56–5.82)
FNH	1.67 ± 0.36 (1.34–2.00)
HCC	1.03 ± 0.43 (0.45–2.45)
Metastasis	1.02 ± 0.28 (0.18–1.46)
Early hepatocellular carcinoma	0.92

Data are means ± 1 standard deviation. Numbers in parentheses are ranges. DDC, distributed diffusion coefficient; FNH, focal nodular hyperplasia; HCC, hepatocellular carcinoma.

Discussion

This study demonstrated the feasibility of using the stretched exponential DWI model for differentiating between benign and malignant hepatic lesions. The malignant hepatic lesions had significantly lower ADC and DDC values than the benign hepatic lesions, and ADC and DDC values showed the highest diagnostic performance for differentiating benign and malignant hepatic lesions, followed by D. Conversely, α did not differ significantly between benign and malignant hepatic lesions. Previous studies concluded that DDC value has the highest diagnostic performance for differentiating benign and malignant hepatic lesions among DWI parameters.[6,17] In contrast, diagnostic performance in DDC values was almost same as that in ADC values in our study.

The parameter DDC values can be considered as summing up the continuous distribution part of each ADC value, weighted by the volume fraction of water molecules. Thus, DDC values represents a theoretically more accurate depiction than ADC value of diffusion in the presence of multi-exponential decay.[9,18] Our results indicated that the average diffusion rate for malignant hepatic lesions was lower than

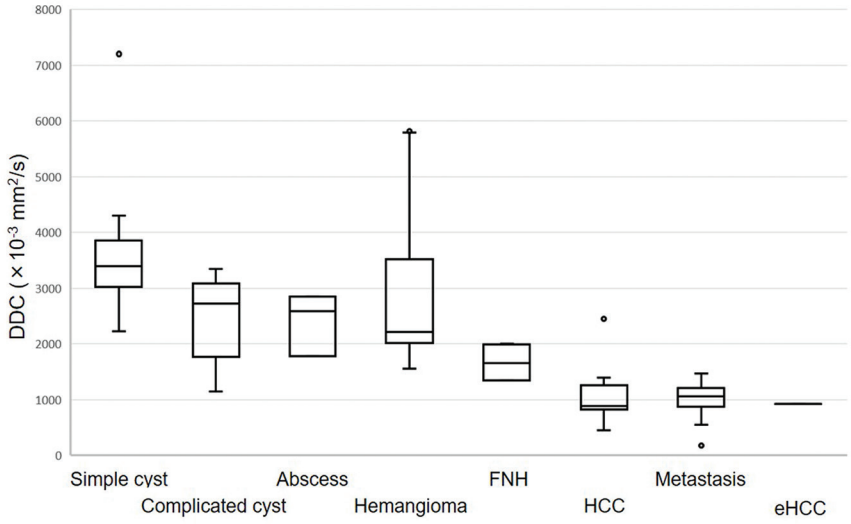

Fig. 2 Box plot showing the DDC values for focal hepatic lesions. These were significantly lower for malignant hepatic lesions than for benign hepatic lesions. DDC, distributed diffusion coefficient; FNH, focal nodular hyperplasia; HCC, hepatocellular carcinoma; eHCC, early hepatocellular carcinoma.

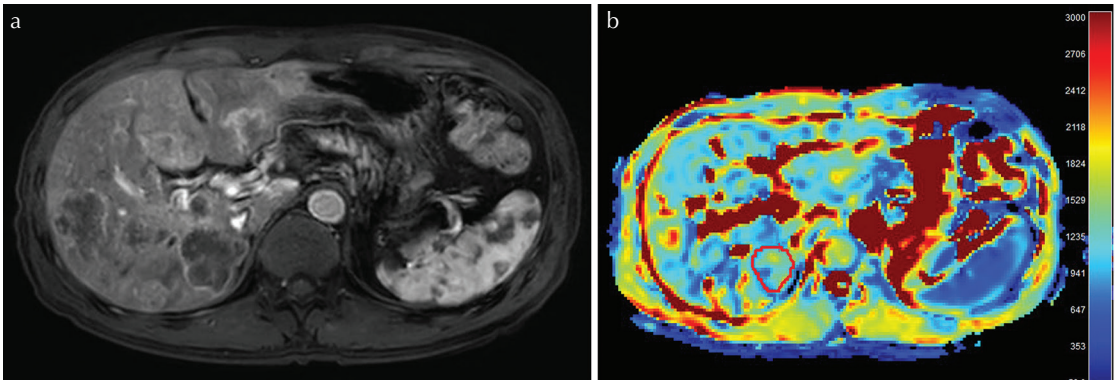

Fig. 3 (**a**) Hepatic arterial dominant phase image and (**b**) DDC map for a 45-year-old man with multiple liver metastases from rectal cancer. The DDC value for the liver metastasis was 1.26×10^{-3} mm^2/s. DDC, distributed diffusion coefficient.

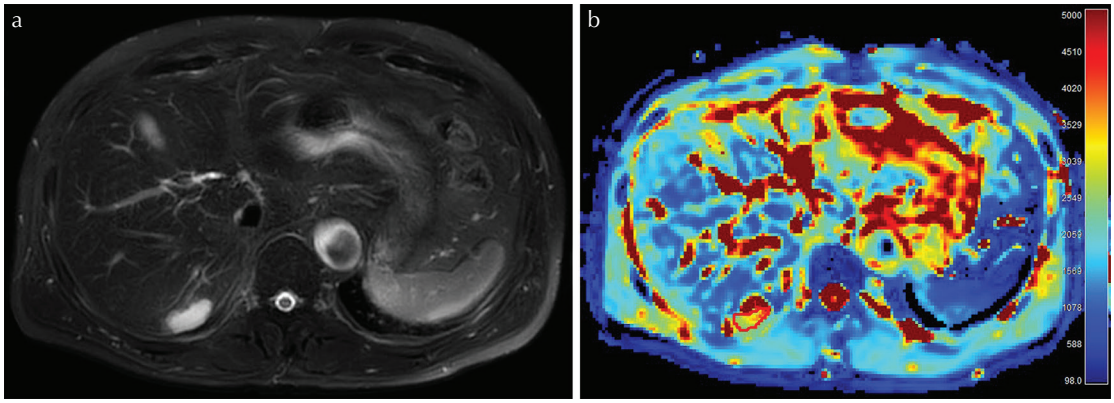

Fig. 4 (**a**) T_2-weighted image and (**b**) DDC map for a 65-year-old man with hemangioma in segment VII. The DDC value for the hemangioma was 2.85×10^{-3} mm^2/s. DDC, distributed diffusion coefficient.

that for benign hepatic lesions. The lower DDC values for malignant lesions may be the result of a higher density of cells and stroma, which restricts the movement of water in the tissue.[7] It is therefore reasonable that DDC values were significantly lower for the malignant hepatic lesions compared to the benign hepatic lesions. In contrast, α, another parameter from the stretched exponential model, did not differentiate benign and malignant hepatic lesions. This parameter represents intravoxel water molecular diffusion heterogeneity. Both benign and malignant hepatic lesions comprise many cell components; we believe there was therefore no significant difference in values of α between benign and malignant hepatic lesions.

Apparent diffusion coefficient and DDC values showed similar diagnostic performance for differentiating benign and malignant hepatic lesions. In a study of prostate cancer, DDC values were higher than ADC values in normal tissue, but lower in prostate cancer tissue, with a relatively higher divergence of up to 13%.[7] The difference in DDC values between normal and prostate cancer tissue was larger than that for ADC values. In the present study, the mean ADC values for benign and malignant hepatic lesions were 2.83×10^{-3} and 1.09×10^{-3} mm^2/s, respectively, whereas the mean DDC values were 3.00×10^{-3} and 1.03×10^{-3} mm^2/s; thus, the differences in mean values between benign and malignant hepatic lesions were 1.74×10^{-3} mm^2/s for ADC values and 1.97×10^{-3} mm^2/s for DDC values. Although the difference in DDC values tended to be greater than that for ADC values, there was no significant difference between ADC and DDC values. In fact, the diagnostic performance for differentiating benign and malignant hepatic lesions was comparable between ADC and DDC values in the present study.

Our study had several limitations. First, the sample size was relatively small, which might have resulted in selection bias. There were few or no solid benign hepatic lesions such as FNH or hepatic adenoma. Moreover, majority of benign hepatic lesions were simple cyst and this can affect the results. The ADC and DDC values for simple cyst are much higher than the other hepatic lesions because it may be the results of a lower density of cells and stroma. Second, we excluded focal hepatic lesions <10 mm in maximum diameter because the software was unable to calculate DWI parameters for these. Third, we did not assess interobserver variability in DWI parameters among the multi-readers. Finally, we did not obtain histopathological confirmation of the lesions. Further prospective analyses with a larger number of patients are needed to confirm our results.

In conclusion, the DDC values obtained from the stretched exponential model gave high AUC for differentiating benign and malignant hepatic lesions. DDC values could be also used as a quantitative imaging biomarker for assessing focal hepatic lesions, however, the diagnostic performance was comparable with ADC values.

Conflicts of Interest

There is no relevant conflicts of interest to disclose.

References

1. Parikh T, Drew SJ, Lee VS, et al. Focal liver lesion detection and characterization with diffusion-weighted MR imaging: comparison with standard breath-hold T_2-weighted imaging. Radiology 2008; 246:812–822.
2. Gourtsoyianni S, Papanikolaou N, Yarmenitis S, Maris T, Karantanas A, Gourtsoyiannis N. Respiratory gated diffusion-weighted imaging of the liver: value of apparent diffusion coefficient measurements in the differentiation between most commonly encountered benign and malignant focal liver lesions. Eur Radiol 2008; 18: 486–492.
3. Bruegel M, Holzapfel K, Gaa J, et al. Characterization of focal liver lesions by ADC measurements using a respiratory triggered diffusion-weighted single-shot echo-planar MR imaging technique. Eur Radiol 2008; 18: 477–485.
4. Choi IY, Lee SS, Sung YS, et al. Intravoxel incoherent motion diffusion-weighted imaging for characterizing focal hepatic lesions: correlation with lesion enhancement. J Magn Reson Imaging 2017; 45:1589–1598.
5. Liu C, Wang K, Li X, et al. Breast lesion characterization using whole-lesion histogram analysis with stretched-exponential diffusion model. J Magn Reson Imaging 2018; 47:1701–1710.
6. Kim HC, Seo N, Chung YE, Park MS, Choi JY, Kim MJ. Characterization of focal liver lesions using the stretched exponential model: comparison with monoexponential and biexponential diffusion-weighted magnetic resonance imaging. Eur Radiol 2019; 29:5111–5120.
7. Liu X, Zhou L, Peng W, Wang H, Zhang Y. Comparison of stretched-exponential and monoexponential model diffusion-weighted imaging in prostate cancer and normal tissues. J Magn Reson Imaging 2015; 42: 1078–1085.
8. Wu Q, Zheng D, Shi L, Liu M, Wang M, Shi D. Differentiating metastatic from nonmetastatic lymph nodes in cervical cancer patients using monoexponential, biexponential, and stretched exponential diffusion-weighted MR imaging. Eur Radiol 2017; 27:5272–5279.
9. Bennett KM, Schmainda KM, Bennett RT, Rowe DB, Lu H, Hyde JS. Characterization of continuously distributed cortical water diffusion rates with a stretched-exponential model. Magn Reson Med 2003; 50:727–734.
10. Bruix J, Sherman M; American Association for the Study of Liver Diseases. Management of hepatocellular carcinoma: an update. Hepatology 2011; 53:1020–1022.
11. Danet IM, Semelka RC, Leonardou P, et al. Spectrum of MRI appearances of untreated metastases of the liver. AJR Am J Roentgenol 2003; 181:809–817.
12. Sano K, Ichikawa T, Motosugi U, et al. Imaging study of early hepatocellular carcinoma: usefulness of gadoxetic acid-enhanced MR imaging. Radiology 2011; 261: 834–844.

13. Seale MK, Catalano OA, Saini S, Hahn PF, Sahani DV. Hepatobiliary-specific MR contrast agents: role in imaging the liver and biliary tree. Radiographics 2009; 29:1725–1748.
14. Qian LJ, Zhu J, Zhuang ZG, Xia Q, Liu Q, Xu JR. Spectrum of multilocular cystic hepatic lesions: CT and MR imaging findings with pathologic correlation. Radiographics 2013; 33:1419–1433.
15. Le Bihan D, Breton E, Lallemand D, Aubin ML, Vignaud J, Laval-Jeantet M. Separation of diffusion and perfusion in intravoxel incoherent motion MR imaging. Radiology 1988; 168:497–505.
16. Hanley JA, McNeil BJ. A method of comparing the areas under receiver operating characteristic curves derived from the same cases. Radiology 1983; 148:839–843.
17. Hu Y, Tang H, Li H, et al. Assessment of different mathematical models for diffusion-weighted imaging as quantitative biomarkers for differentiating benign from malignant solid hepatic lesions. Cancer Med 2018; 7:3501–3509.
18. Kwee TC, Galbán CJ, Tsien C, et al. Comparison of apparent diffusion coefficients and distributed diffusion coefficients in high-grade gliomas. J Magn Reson Imaging 2010; 31: 531–537.